Figure S1

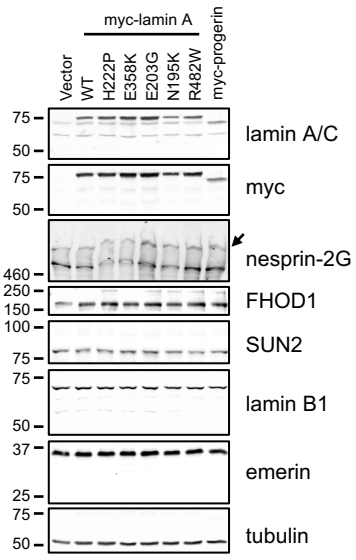
myc-lamin A
Vector
WT
H222P
E358K
E203G
N195K
R482W
myc-progerin
75
50
lamin A/C
75
50
myc
460
250
150
nesprin-2G
FHOD1
100
75
SUN2
75
50
lamin B1
37
25
emerin
75
50
tubulin

Figure S2

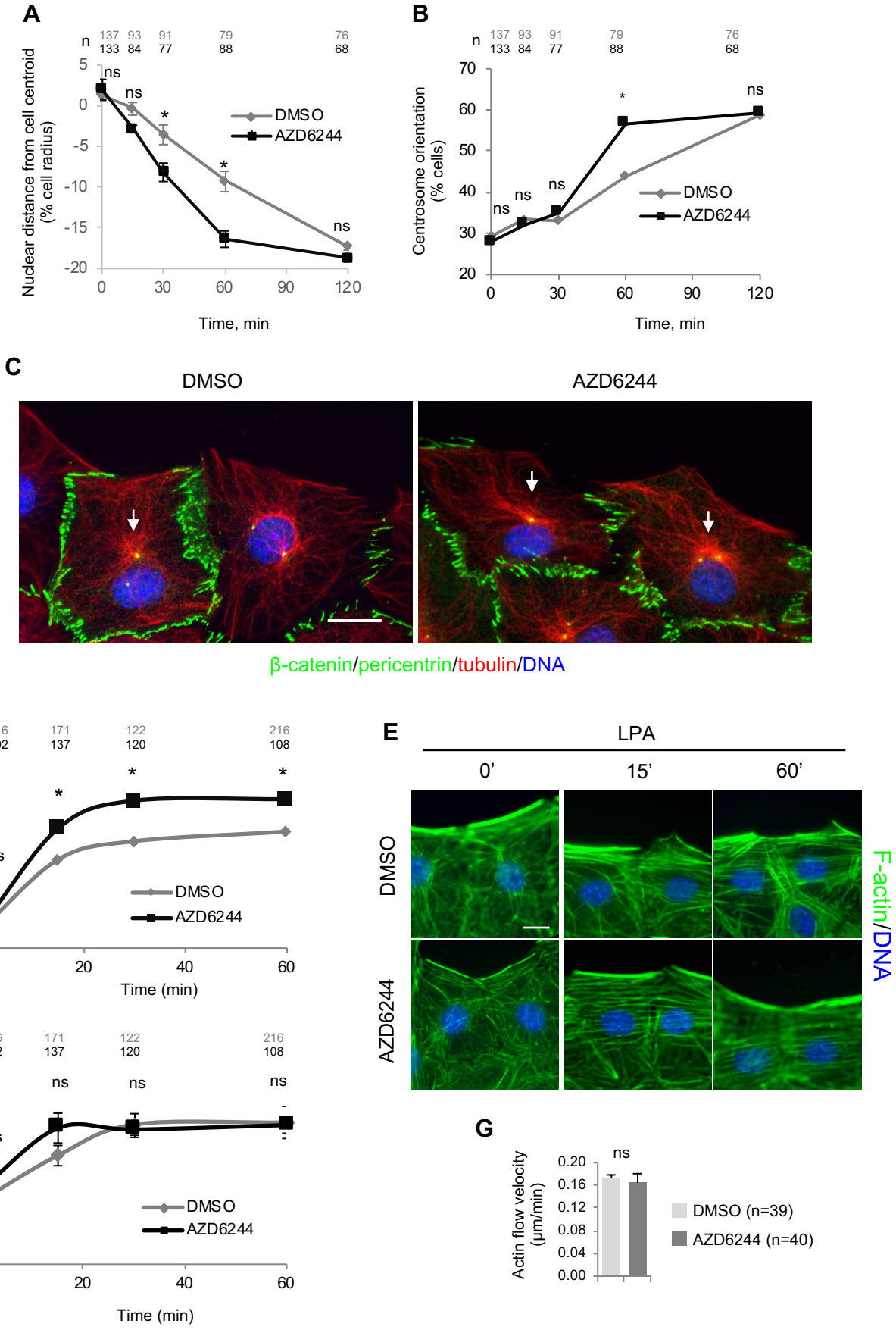
A
n 137 93 91 79 76
133 84 77 88 68
Nuclear distance from cell centroid (% cell radius)
Time, min
DMSO
AZD6244
ns
*
B
Centrosome orientation (% cells)
Time, min
C
DMSO
AZD6244
β-catenin/pericentrin/tubulin/DNA
D
% cells with TAN line
Time (min)
n 116 171 122 216
92 137 120 108
E
LPA
0’
15’
60’
DMSO
AZD6244
F-actin/DNA
F
Average # of actin cable over nucleus
Time (min)
G
Actin flow velocity (μm/min)
DMSO (n=39)
AZD6244 (n=40)

Figure S3

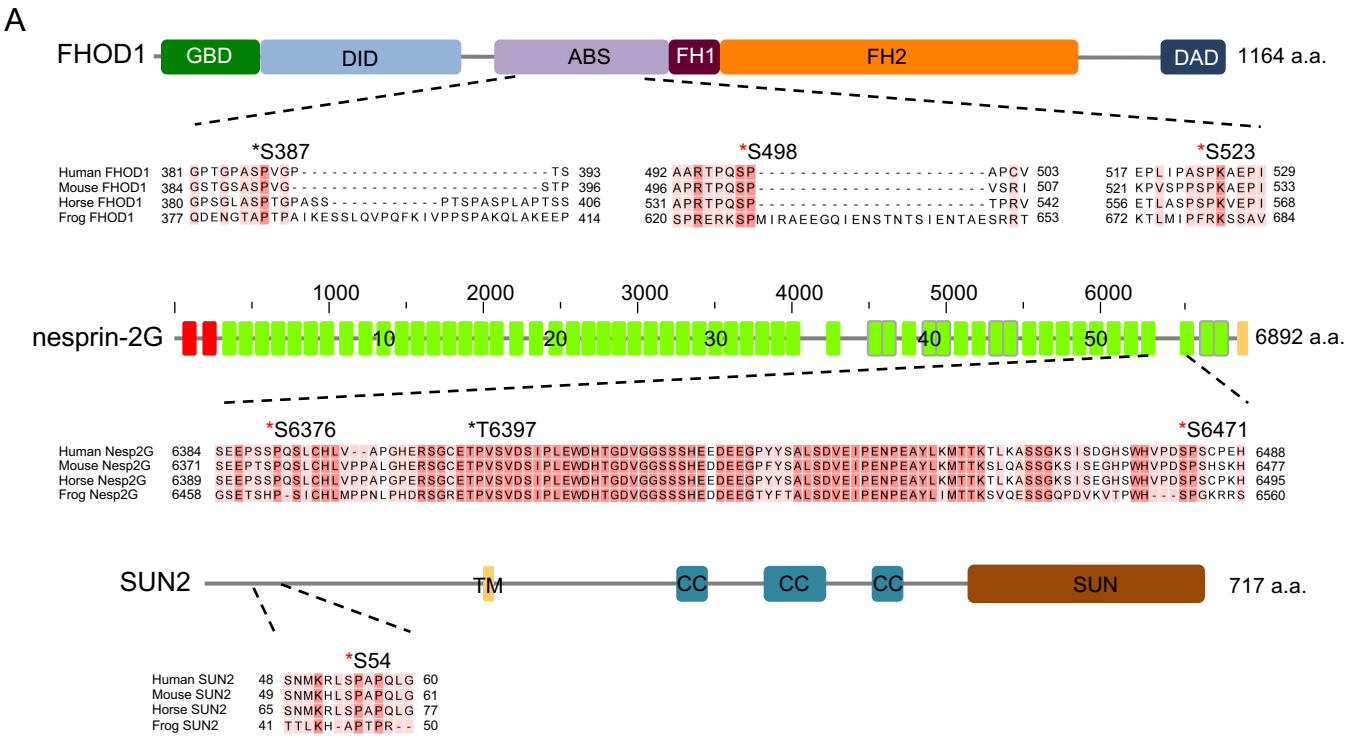
A
FHOD1
GBD
DID
ABS
FH1
FH2
DAD
1164 a.a.
*S387
*S498
*S523
Human FHOD1 381 GPTGPASPVGP----------TS 393
Mouse FHOD1 384 GSTGSASPVG----------STP 396
Horse FHOD1 380 GPSGLASPTGPASS----------PTSPASPLAPTSS 406
Frog FHOD1 377 QDENGTAPTPAIKESSLQVPQFKIVPPSPAKQLAKEEP 414
492 AARTPQSP----------APCV 503
496 APRTPQSP----------VSRI 507
531 APRTPQSP----------TPRV 542
620 SPRERKSPMIRAEEGQIENSTNTSIENTAESRRT 653
517 EPLIPASPKAEPI 529
521 KPVSPPSPKAEPI 533
556 ETLASPSPKVEPI 568
672 KTLMIPFRKSSAV 684
1000
2000
3000
4000
5000
6000
nesprin-2G
10
20
30
40
50
6892 a.a.
*S6376
*T6397
*S6471
Human Nesp2G 6384 SEEPSSPQSLCHLV--APGHERSGCETPVSVDSIPLEWDHTGDVGGSSSHEEDEEGPYYSALSDVEIPENPEAYLKMTTKTLKASSGKSISDGHSWHVPDSPSCPEH 6488
Mouse Nesp2G 6371 SEEPTSPQSLCHLVPPALGHERSGCETPVSVDSIPLEWDHTGDVGGSSSHEDDEEGPFYSALSDVEIPENPEAYLKMTTKSLQASSGKSISEGHPWHVPDSPSHSKH 6477
Horse Nesp2G 6389 SEEPSSPQSLCHLVPPAPGPERSGCETPVSVDSIPLEWDHTGDVGGSSSHEEDEEGPYYSALSDVEIPENPEAYLKMTTKTLKASSGKSISEGHSWHVPDSPSCPKH 6495
Frog Nesp2G 6458 GSETSHP-SICHLMPPNLPHDRSGRETPVSVDSIPLEWDHTGDVGGSSSHEDDEEGTYFTALSDVEIPENPEAYLIMTTKSVQESSGQPDVKVTPWH---SPGKRRS 6560
SUN2
TM
CC
CC
CC
SUN
717 a.a.
*S54
Human SUN2 48 SNMKRLSPAPQLG 60
Mouse SUN2 49 SNMKHLSPAPQLG 61
Horse SUN2 65 SNMKRLSPAPQLG 77
Frog SUN2 41 TTLKH-APTPR-- 50

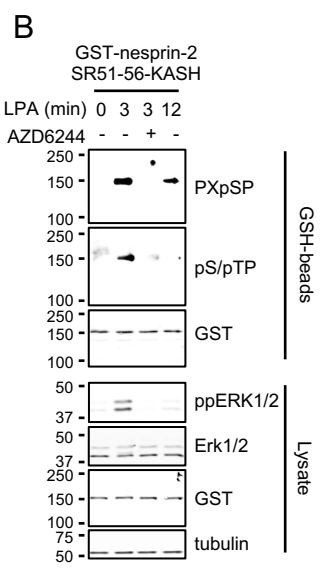
B
GST-nesprin-2
SR51-56-KASH
LPA (min) 0 3 3 12
AZD6244 - - + -
250
150
100
PXpSP
250
150
100
pS/pTP
250
150
100
GST
GSH-beads
50
37
ppERK1/2
50
37
Erk1/2
250
150
100
GST
75
50
tubulin
Lysate

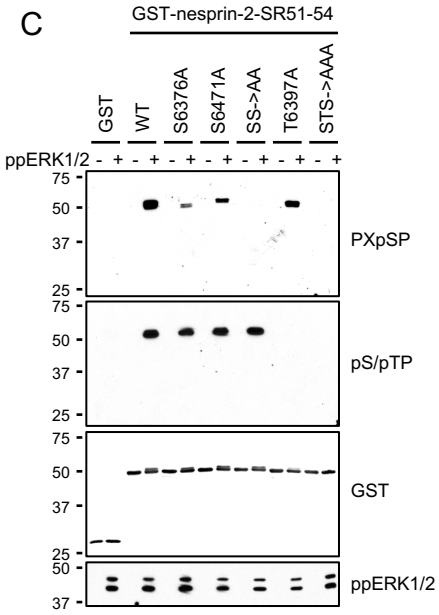
C
GST-nesprin-2-SR51-54
GST
WT
S6376A
S6471A
SS->AA
T6397A
STS->AAA
ppERK1/2 - + - + - + - + - + - + - +
75
50
37
25
PXpSP
75
50
37
25
pS/pTP
75
50
37
25
GST
50
37
ppERK1/2

Figure S4

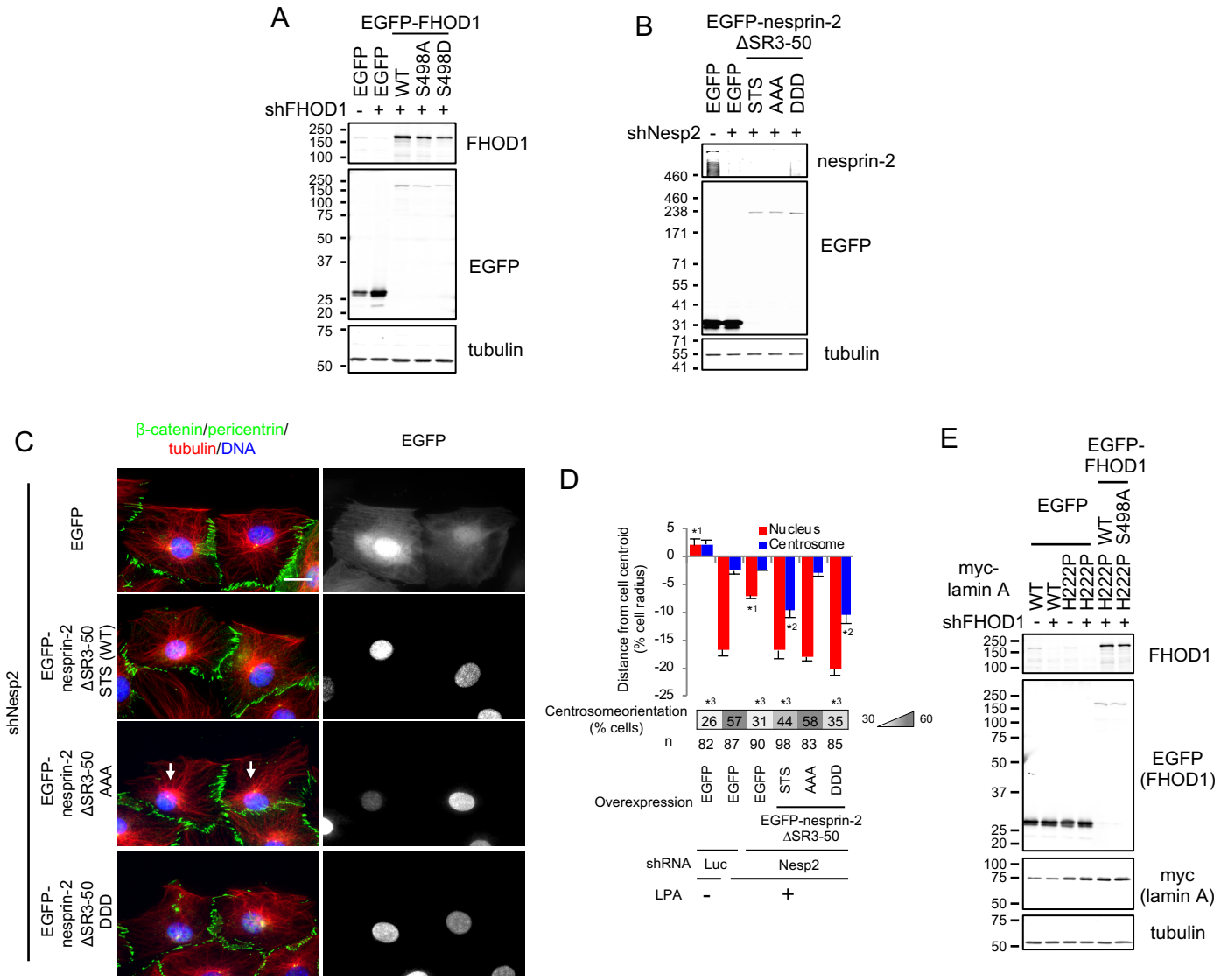
A
EGFP-FHOD1
EGFP
EGFP
WT
S498A
S498D
shFHOD1 - + + + +
250
150
100
FHOD1
250
150
100
75
50
37
25
20
EGFP
75
50
tubulin
B
EGFP-nesprin-2 ΔSR3-50
EGFP
EGFP
STS
AAA
DDD
shNesp2 - + + + +
460
nesprin-2
460
238
171
71
55
41
31
EGFP
71
55
41
tubulin
C
β-catenin/pericentrin/
tubulin/DNA
EGFP
shNesp2
EGFP
EGFP-nesprin-2 ΔSR3-50 STS (WT)
EGFP-nesprin-2 ΔSR3-50 AAA
EGFP-nesprin-2 ΔSR3-50 DDD
D
Distance from cell centroid (% cell radius)
5
0
-5
-10
-15
-20
-25
Nucleus
Centrosome
*1
*1
*2
*2
*3
*3
*3
*3
Centrosomeorientation (% cells)
26
57
31
44
58
35
30
60
n
82
87
90
98
83
85
Overexpression
EGFP
EGFP
EGFP
STS
AAA
DDD
EGFP-nesprin-2 ΔSR3-50
shRNA
Luc
Nesp2
LPA
-
+
E
EGFP-FHOD1
EGFP
WT
S498A
myc-lamin A
WT
WT
H222P
H222P
H222P
shFHOD1 - + - + + +
250
150
100
FHOD1
250
150
100
75
50
37
25
20
EGFP (FHOD1)
100
75
50
myc (lamin A)
75
50
tubulin

Figure S5

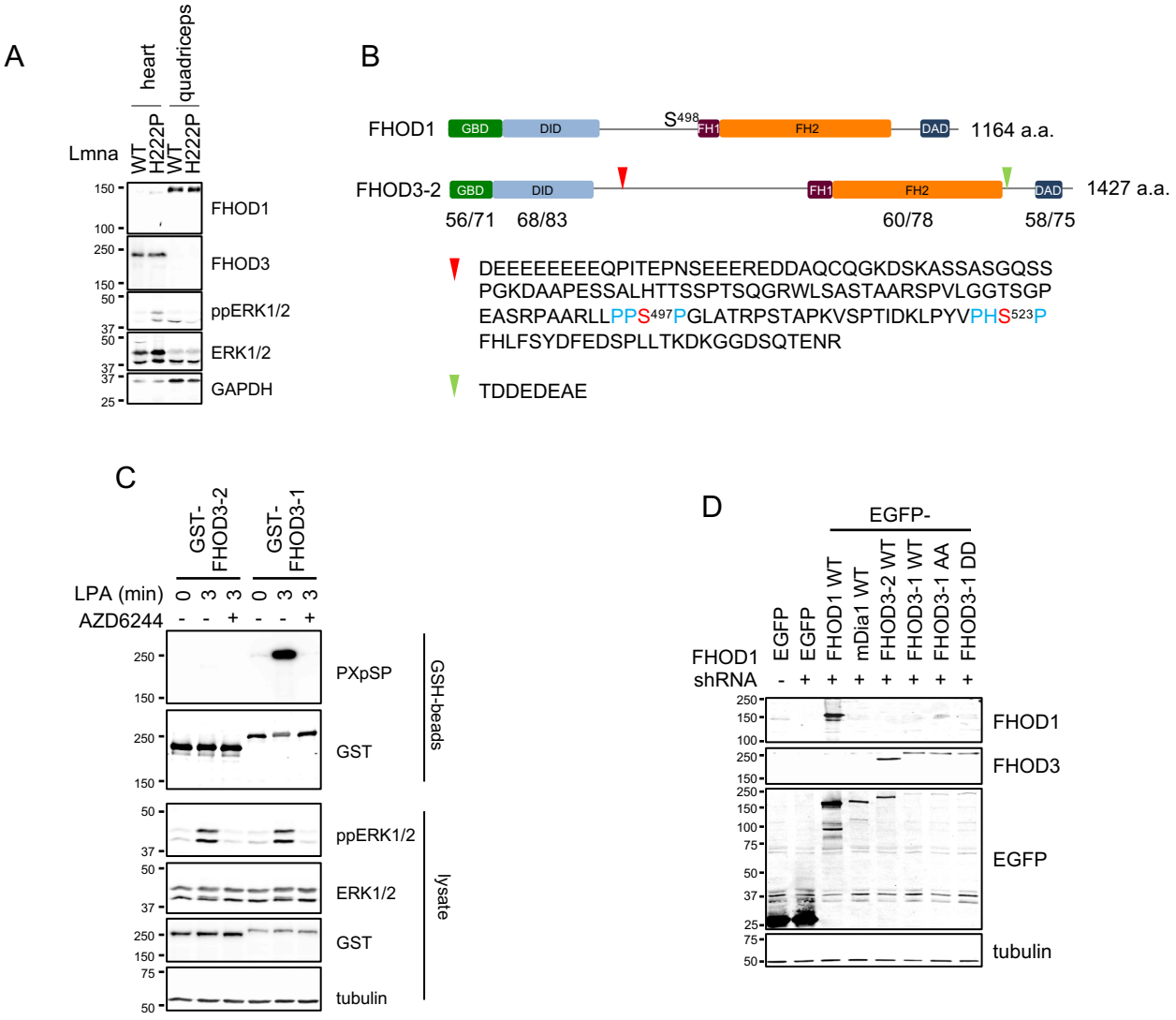
A
heart
quadriceps
Lmna
WT
H222P
WT
H222P
150
100
250
150
50
37
50
37
37
25
FHOD1
FHOD3
ppERK1/2
ERK1/2
GAPDH
B
FHOD1
GBD
DID
S498
FH1
FH2
DAD
1164 a.a.
FHOD3-2
GBD
DID
FH1
FH2
DAD
1427 a.a.
56/71
68/83
60/78
58/75
DEEEEEEEEQPITEPNSEEEREDDAQCQGKDSKASSASGQSS
PGKDAAPESSALHTTSSPTSQGRWLSASTAARSPVLGGTSGP
EASRPAARLLPPS497PGLATRPSTAPKVSPTIDKLPYVPHS523P
FHLFSYDFEDSPLLTKDKGGDSQTENR
TDDEDEAE
C
GST-FHOD3-2
GST-FHOD3-1
LPA (min)
0
3
3
0
3
3
AZD6244
-
-
+
-
-
+
250
150
250
150
50
37
50
37
250
150
75
50
PXpSP
GST
ppERK1/2
ERK1/2
GST
tubulin
GSH-beads
lysate
D
EGFP-
FHOD1 shRNA
EGFP
EGFP
FHOD1 WT
mDia1 WT
FHOD3-2 WT
FHOD3-1 WT
FHOD3-1 AA
FHOD3-1 DD
-
+
+
+
+
+
+
+
250
150
100
250
150
250
150
100
75
50
37
25
75
50
FHOD1
FHOD3
EGFP
tubulin

Figure S6

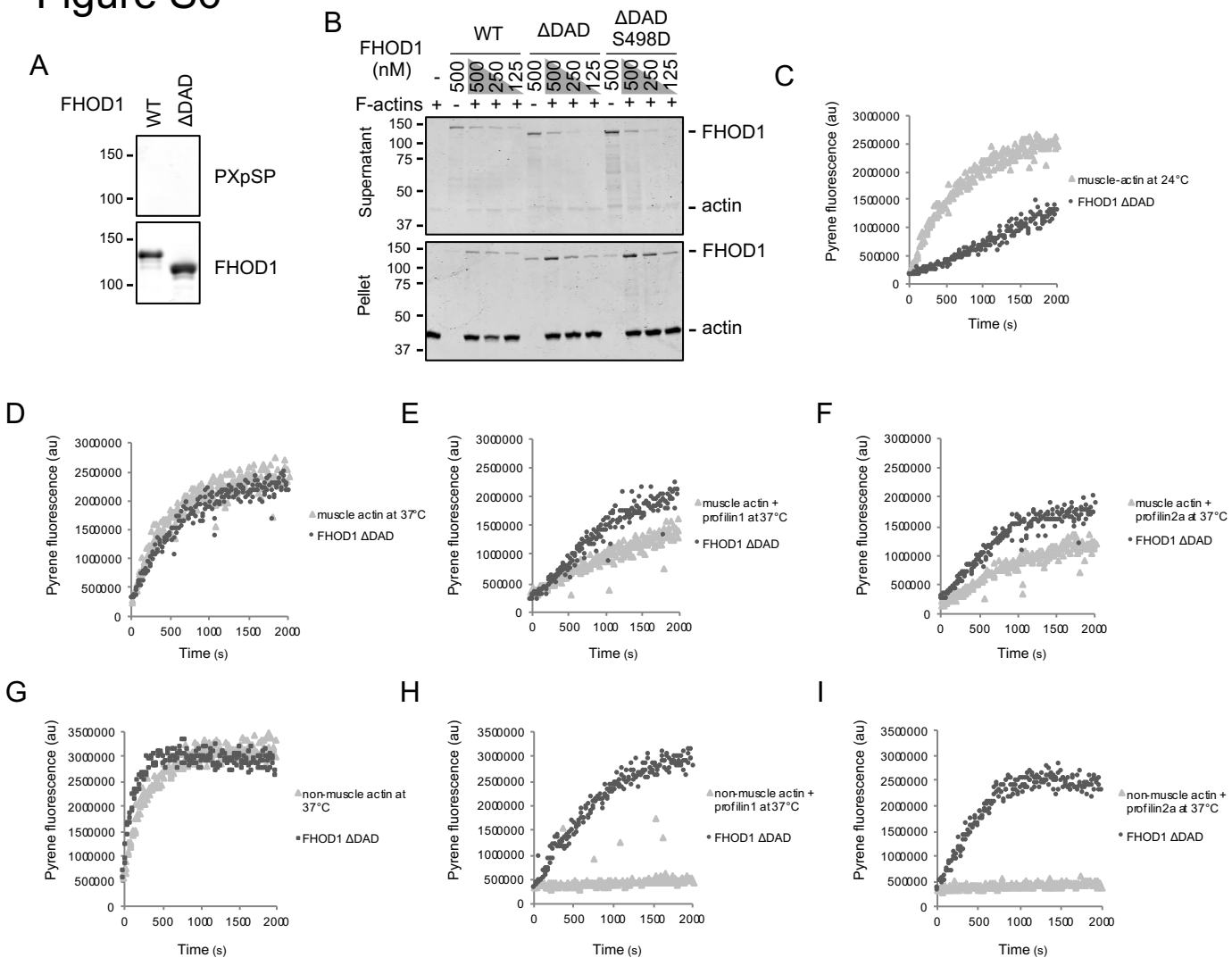
A
FHOD1
WT
ΔDAD
150
100
PXpSP
150
100
FHOD1
B
FHOD1 (nM)
WT
ΔDAD
ΔDAD S498D
-
500
500
250
125
500
500
250
125
500
500
250
125
F-actins + - + + + - + + + - + + +
Supernatant
150
100
75
50
37
FHOD1
actin
Pellet
150
100
75
50
37
FHOD1
actin
C
Pyrene fluorescence (au)
3000000
2500000
2000000
1500000
1000000
500000
0
0 500 1000 1500 2000
Time (s)
muscle-actin at 24°C
FHOD1 ΔDAD
D
Pyrene fluorescence (au)
Time (s)
muscle actin at 37°C
FHOD1 ΔDAD
E
Pyrene fluorescence (au)
Time (s)
muscle actin + profilin1 at 37°C
FHOD1 ΔDAD
F
Pyrene fluorescence (au)
Time (s)
muscle actin + profilin2a at 37°C
FHOD1 ΔDAD
G
Pyrene fluorescence (au)
3500000
3000000
2500000
2000000
1500000
1000000
500000
0
0 500 1000 1500 2000
Time (s)
non-muscle actin at 37°C
FHOD1 ΔDAD
H
Pyrene fluorescence (au)
Time (s)
non-muscle actin + profilin1 at 37°C
FHOD1 ΔDAD
I
Pyrene fluorescence (au)
Time (s)
non-muscle actin + profilin2a at 37°C
FHOD1 ΔDAD

Figure S7

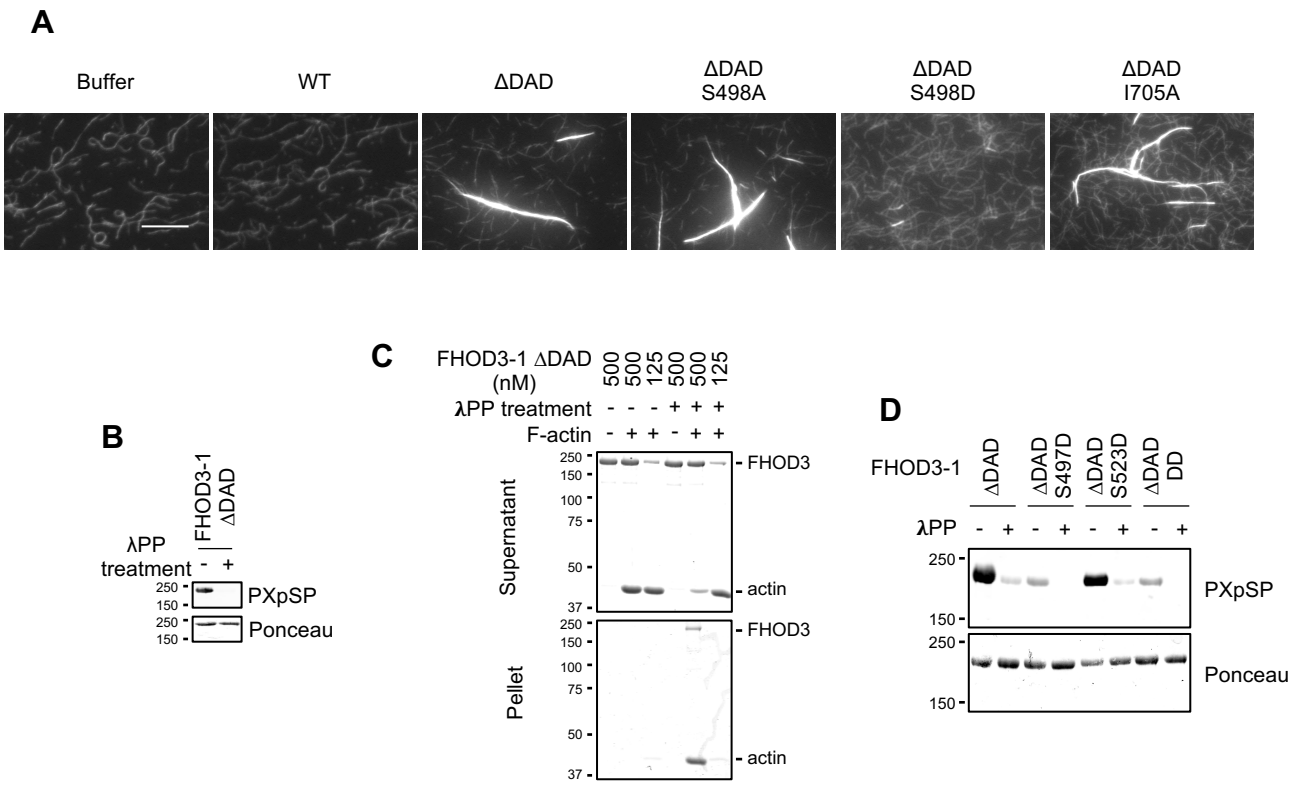
A
Buffer
WT
ΔDAD
ΔDAD S498A
ΔDAD S498D
ΔDAD I705A
B
FHOD3-1 ΔDAD
λPP treatment - +
250
150
PXpSP
250
150
Ponceau
C
FHOD3-1 ΔDAD (nM) 500 500 125 500 500 125
λPP treatment - - - + + +
F-actin - + + - + +
Supernatant
250
150
100
75
50
37
FHOD3
actin
Pellet
250
150
100
75
50
37
FHOD3
actin
D
FHOD3-1 ΔDAD ΔDAD S497D ΔDAD S523D ΔDAD DD
λPP - + - + - + - +
250
150
PXpSP
250
150
Ponceau

SUPPLEMENTAL INFORMATION

Figure S1. Expression of lamin A variants, related to Figure 2.

Western blots of NIH3T3 fibroblasts expressing the indicated myc-lamin A constructs. Antibodies used to probe the blots are indicated on the right. Arrow denotes nesprin-2G ; lower band is likely non-specific staining as only the top band was reduced by shRNA targeting nesprin-2G.Tubulin is a loading control. Migration of molecular mass (kDa) standards is shown at the left.

Figure S2. Nuclear movement, TAN line formation, and Actin cable formation of NIH3T3 fibroblast cells treated with MEK1/2 inhibitor AZD6244, related to Figure 3.

(A) Time course of nuclear displacement in LPA-stimulated NIH3T3 fibroblasts treated with vehicle (DMSO) or AZD6244. Values are means ± SEM; n, cell examined. *$p < 0.05$; ns, $p > 0.05$. (B) Time course of centrosome orientation of NIH3T3 fibroblasts treated with DMSO or AZD6244 after LPA stimulation. Values are means ± SEM; n, cells examined. *$p < 0.05$. (C) Images of LPA-stimulated wound-edge NIH3T3 fibroblasts treated with DMSO or AZD6244 and stained for the indicated proteins and DAPI. Arrows, oriented centrosomes. Bar, 20 μm. (D) Time course of TAN line formation in NIH3T3 fibroblasts stimulated with LPA and treated with vehicle (DMSO) or AZD6244. Values are means ± SEM; n, cells examined. *$p < 0.05$; ns, $p > 0.05$. (E) Images of LPA-stimulated wound-edge NIH3T3 fibroblasts treated with DMSO or AZD6244 and stained with fluorescently conjugated phalloidin (F-actin) and DAPI (DNA). Bar, 20 μm. (F) Time course of actin cable formation over the nucleus in NIH3T3 fibroblasts stimulated with LPA and treated with vehicle (DMSO) or AZD6244. Values

are means ± SEM; n, cells examined. *p < 0.05; ns, p > 0.05. (G) Velocity of actin cable flow after LPA stimulation of NIH3T3 fibroblasts treated with vehicle (DMSO) or AZD6244. Values are means ± SEM; n, cells examined. ns, p > 0.05.

Figure S3. Predicted consensus ERK1/2 phosphorylation sites in TAN line components and evidence for nesprin-2 phosphorylated by ERK1/2, related to Figure 4.

(A) Schematics of FHOD-1, nesprin-2G, and SUN2 and predicted ERK1/2 phosphorylation sites. Domains of FHOD1 and nesprin-2G are described in the legend to Figure 4. SUN2 domains are transmembrane membrane (TM), coiled-coil (CC) and the SUN domain (SUN). The sequence alignments below the protein diagrams depict the sequence homology among various species, with sequence conservation indicated by red (high), pink (moderate) and white (low). (B) Western blots of lysates of NIH3T3 fibroblasts expressing GST-nesprin-2-SR51-56-KASH construct probed with the antibodies indicated on the right. GST proteins were captured on GSH-beads before western blotting. Time after LPA stimulation and treatment with AZD6244 is indicated at the top of each lane. Tubulin is a loading control. (C) Western blots of GST or GST-nesprin-2-SR51-54 fusion proteins incubated without (-) or with (+) immunoprecipitated active ERK1/2 kinases (ppERK1/2) in the presence of ATP. Antibodies used to probe the blots are indicated on the right. GST-nesprin-2-SR51-54 SS->AA carries S6376A and S6471A mutations; STS->AAA carries S6376A, T6397A and S6471A mutations.
In B and C, migration of molecular mass standards (kDa) is indicated at the left of each blot.

Figure S4. Expression levels of nesprin-2 ΔSR3-50 and FHOD1 mutants in nesprin-2 or FHOD1 knockdown NIH3T3 fibroblasts and NIH3T3 fibroblasts expressing lamin A H222P, related to Figure 5.

(A) Western blots of lysates of NIH3T3 fibroblasts with or without FHOD1 shRNA (shFHOD1) expression and expressing either EGFP or EGFP-tagged FHOD1 proteins. Antibodies used to probe the blots are indicated on the right. (B) Western blots of lysates of NIH3T3 fibroblasts with or without nesprin-2 shRNA (shNesp2) expression and expressing either EGFP or EGFP-tagged nesprin-2 ΔSR3-50 proteins. Antibodies used to probe the blots are indicated on the right. EGFP-nesprin-2 ΔSR3-50 STS carries no mutation on S6376, T6397, and S6471; AAA carries S6376A, T6397A and S6471A mutations; and DDD carries S6376D, T6397D and S6471D mutations. (C) Images of LPA-stimulated wound-edge NIH3T3 fibroblasts expressing EGFP or EGFP-tagged nesprin-2 ΔSR3-50 proteins after knockdown of nesprin-2 and stained for the indicated proteins and DAPI. White arrows, oriented centrosomes. Bars, 20 μm. (D) Centrosome and nuclear position and centrosome orientation for the cells treated as in A. Values are means ± SEM; n, cells examined. Centrosome orientation (mean % of cells), is shown in the heat map below the histograms. $*^1$ and $*^2$ indicate $p < 0.05$ compared to the rest of the samples for each category. $*^3$ indicates $p < 0.05$ compared to the LPA-stimulated control. (E) Western blots of lysates of NIH3T3 fibroblasts transfected with or without shRNA to knockdown endogenous FHOD1 (shFHOD1) and re-expressing either EGFP or EGFP-tagged FHOD1 as well as myc-tagged WT lamin A or lamin A H222P. Antibodies used to probe the blots are indicated on the right.

In A, B, and E, migration of molecular mass standards (kDa) is shown at the left of each blot.

Figure S5. ERK1/2-catalyzed phosphorylation of the cardiac form of FHOD3, related to Figure 6.

(A) Western blots of lysates from heart and quadriceps of 20-week-old WT and *Lmna*$^{H222P/H222P}$ (H222P) male mice probed with antibodies indicated on the right.

(B) Schematics of mouse FHOD1 and FHOD3. Domains are the same as those described for FHOD1 in the legend to Figure 4. The numbers below indicate the identity/similarity of each domain between human FHOD1 and mouse FHOD3. Red and green arrowheads indicate the sites of the two inserts in the cardiac form of mouse FHOD3, FHOD3-1. Sequences of the FHOD3-1 inserts are given below. (C) Western blots of lysates of NIH3T3 fibroblasts expressing GST-FHOD3-2 and FHOD3-1 probed with the antibodies indicated on the right. GST proteins were captured on GSH-beads before western blotting. Time after LPA stimulation and treatment with AZD6244 is indicated at the top of each lane. (D) Western blots of lysates of NIH3T3 fibroblasts transfected with or without shRNA transfection to knock down endogenous FHOD1 (shFHOD1) and re-expressing the indicated proteins. FHOD3-1 DD carries S497D and S523D mutations. Blots were probed using the antibodies indicated on the right.

In A, C, and D, migration of molecular mass standards (kDa) is shown at the left of each blot.

Figure S6. The active form of FHOD1 stimulates polymerization of muscle and non-muscle actin in the presence of profilin, related to Figure 7.

(A) Western blots of WT and FHOD1 ΔDAD proteins isolated from 293T cells and probed with antibodies against PXpSP or FHOD1. Migration of molecular mass standards (kDa) is indicated at the left of each blot. (B) Actin binding activity of FHOD1 proteins examined using a high-speed (100,000 x *g*) actin co-sedimentation assay. Coomassie blue-stained SDS-polyacrylamide gels of proteins in the supernatant and pellet are shown. F-actin concentration was 2 μM; FHOD1 protein concentration is as indicated. Migration of molecular mass standards (kDa) is indicated at the left. (C-F) Polymerization of rabbit skeletal muscle actin by the activated form of FHOD1 (FHOD1 ΔDAD) measured by a pyrene-actin polymerization assay. 2 μM muscle actin (10% pyrene-labeled) was pre-incubated with no profilin (C and D), 4 μM human profilin1 (E) or profilin2a (F). Polymerized was initiated in the presence or absence of 50 nM FHOD1 ΔDAD at 24 ºC (C) or 37ºC (D-F). (G-I) Polymerization of human platelet non-muscle actin by FHOD1 ΔDAD measured by a pyrene-actin polymerization assay. 2.5 μM non-muscle actin (10% pyrene-labeled) was pre-incubated with no profilin (G), 5 μM profilin1 (H) or 5 μM profilin2a (I). Polymerization was initiated in the presence or absence of 62.5 nM FHOD1 ΔDAD at 37 ºC.

Figure S7. FHOD1 and FHOD3 stimulate F-actin bundling, related to Figure 7.

(A) TIRF images of Alexa-fluor 488 phalloidin decorated F-actin incubated with indicated purified FHOD1 protein. Note the lack of bundling by the phosphomimetic FHOD1 ΔDAD S498D. Bar, 5 μm. (B) Western blots of purified FHOD3-1 proteins from 293T

cells before and after phosphatase treatment (λPP). Blots were probed with the antibodies indicated in the right. (C) Actin bundling activity of purified FHOD3-1 before and after treatment with phosphatase (λPP) assessed with a low speed actin co-sedimentation assay. Coomassie blue-stained SDS-polyacrylamide gels of proteins in the supernatant and pellet are shown. (D) Western blot of the indicated purified FHOD3-1 proteins before and after phosphatase treatment (λPP) probed with anti-PXpSP antibody. A Ponceau S-stained blot is shown under the antibody probed blot. FHOD3-1 ΔDAD DD is FHOD3-1 ΔDAD S497D S523D. In B, C, and D, migration of molecular mass standards (kDa) is indicated at the left of each blot.